*SAE TECHNICAL PAPER SERIES*

**2002-01-0319**

# The Influence of Damper Properties on Vehicle Dynamic Behaviour

**Adrian Simms and David Crolla**
The University of Leeds, School of Mechanical Engineering

**Reprinted From: Steering and Suspension Technology Symposium 2002 (SP–1654)**

*The Engineering Society For Advancing Mobility Land Sea Air and Space®*
*INTERNATIONAL*

**SAE 2002 World Congress**
**Detroit, Michigan**
**March 4-7, 2002**

**400 Commonwealth Drive, Warrendale, PA 15096-0001 U.S.A. Tel: (724) 776-4841 Fax: (724) 776-5760**

The appearance of this ISSN code at the bottom of this page indicates SAE's consent that copies of the paper may be made for personal or internal use of specific clients. This consent is given on the condition, however, that the copier pay a per article copy fee through the Copyright Clearance Center, Inc. Operations Center, 222 Rosewood Drive, Danvers, MA 01923 for copying beyond that permitted by Sections 107 or 108 of the U.S. Copyright Law. This consent does not extend to other kinds of copying such as copying for general distribution, for advertising or promotional purposes, for creating new collective works, or for resale.

Quantity reprint rates can be obtained from the Customer Sales and Satisfaction Department.

To request permission to reprint a technical paper or permission to use copyrighted SAE publications in other works, contact the SAE Publications Group.

***GLOBAL MOBILITY** DATABASE*

***All SAE papers, standards, and selected books are abstracted and indexed in the Global Mobility Database***

No part of this publication may be reproduced in any form, in an electronic retrieval system or otherwise, without the prior written permission of the publisher.

**ISSN 0148-7191**
**Copyright © 2002 Society of Automotive Engineers, Inc.**

Positions and opinions advanced in this paper are those of the author(s) and not necessarily those of SAE. The author is solely responsible for the content of the paper. A process is available by which discussions will be printed with the paper if it is published in SAE Transactions. For permission to publish this paper in full or in part, contact the SAE Publications Group.

Persons wishing to submit papers to be considered for presentation or publication through SAE should send the manuscript or a 300 word abstract of a proposed manuscript to: Secretary, Engineering Meetings Board, SAE.

**Printed in USA**

2002-01-0319

# The Influence of Damper Properties on Vehicle Dynamic Behaviour

**Adrian Simms and David Crolla**
The University of Leeds, School of Mechanical Engineering

Copyright © 2002 Society of Automotive Engineers, Inc.

## ABSTRACT

This paper details a non-linear hysteretic physical shock absorber model, and the processes utilised to identify the constituent parameters. In the current paper the model parameters are extracted from experimental data for the 'sport' setting of a prototype front shock absorber for a vehicle in the luxury class. The model is validated by comparing simulated results to experimental data for a test damper, for three discrete frequencies of sinusoidal excitation of 1,3 and 12 Hz. Finally the shock absorber model is included in a quarter car vehicle ride model and output characteristics are compared to those obtained with classical damper representations.

## INTRODUCTION

The detailed dynamic properties of dampers are known to influence substantially some of the subtle, and yet nevertheless hugely important, refinement aspects of vehicle ride and handling. However, damper properties are typically characterised by quasi-steady properties for vehicle simulation purposes. The classic 14 speed test [1], for example, involves subjecting a damper to 14 differing frequency levels of fixed amplitude sinusoidal excitation, and then plotting the peak force values obtained versus the relevant test velocity. Such a representation of shock absorber behaviour is clearly deficient for the purpose of vehicle simulations as only a snap shot view of the damper's behaviour is utilised and much information is discarded. As a direct consequence the process of damper valve tuning is still carried out to a great extent via ride work. This consists of ride engineers subjectively rating the performance of the prototype vehicle(s) over a series of test tracks/ride routes. The damper valve is then possibly adjusted to improve the vehicle's ride/handling or to obtain characteristics expected for that class of vehicle. This process is clearly open to subjective evaluation which may vary driver to driver, and even from one day to the next.

A more scientific approach to the issue of damper tuning, via vehicle simulations, would offer a number of significant benefits. This is simply due to the fact that the bulk of the damper selection process could be carried out prior to the manufacture of any vehicle prototypes, and this technique would be far less subjective in nature. Such an approach would necessitate an improved method of characterising the damper, such that the important dynamic features are represented, and comprehension of the links between more subtle features of the damper response. The current paper attempts to address the aforementioned requirement for improved damper characterisation in the context of the 'sport' setting of a triple rate prototype adaptive shock absorber.

## SHOCK ABSORBER MODELLING APPROACH

In order to select the optimum damper modelling strategy for a 'virtual damper tuning environment', the suitability of the differing approaches found within published literature were determined with respect to the following criterion:

- Ability to capture damper non-linearity and dynamic behaviour.
- Flexibility to model different shock absorber types.
- Ease of model generation (Experiment/Parameter identification).
- Suitability for use in vehicle simulations.
- Usefulness as a predictive tool.

Clearly black box methods such as the Restoring Force Mapping method [2-5] and neural networks [6], do not satisfy the need for a predictive tool as they are inherently non-tuneable. The same applies to elementary models constructed with spring and ideal viscous damping elements [7,8]. The required need for tuneable elements for this damper model application lends itself to an explicit physical model, where the damper control force is related to physical parameters that govern the dampers internal flows and pressures.

The high detail model developed by Lang [9,10], for a twin tube shock absorber, was the first physical model that actually aimed to predict damper behaviour over a wide range of operating conditions. This 87 parameter model gave good correlation with experiment, but both simulation and parameter identification processes were highly iterative. It was also very specific to the shock

absorber under investigation. It did however identify the contribution of internal compliance's to the hysteretic nature of dampers.

More recently models by Duym [11-13], Lang and Sonnenburg [14] and Herr et al [16] attempted to generate more readily identifiable physical damper models. Each of these models are similar in overall structure in that they consist of a pressure model(s) and valve pressure/flow characterisations. The pressure models are a selection of first order non-linear differential equations, which are utilised to determine the various internal chamber pressures, and are derived from pressure dependent oil compressibility models. For the pressure/flow model Duym [11-13] identified valve parameters from several simple dynamometer tests and an additional 'incompressible' model (see definitions); these parameters were then used to analytically determine valve flows for given pressure drops in the main model. In contrast Lang and Sonnenburg [15] used experimentally obtained pressure/flow data, and Herr et al evaluated the pressure flow characteristics of the differing valve components using Computational Fluid Dynamics (CFD). In the absence of a large database of pressure/flow data for differing valve formulations, as was available to Lang and Sonnenburg, this non parametric form of pressure model does not satisfy the required criteria of tune-ability. The CFD approach is a time consuming process requiring detailed modelling even for varying damper valves of the same basic architecture. As a result of the aforementioned considerations the damper modelling approach to be taken is one of a physical model similar to that of Duym [11-13].

## SHOCK ABSORBER ARCHITECTURE, AXES SYSTEMS AND SIGN CONVENTIONS

The prototype shock absorber, in the 'sport' setting, falls into the mono-tube category; the only flow paths for the internal hydraulic fluid are thus through the piston's valves (see Figure 1). The additional 'softer' damper settings, which are achieved by the solenoid activation of additional flow paths, will not be considered in this paper. The mono-tube shock absorber consists of a rebound chamber and a compression chamber which are both oil filled. A high pressure nitrogen gas volume, typically 20-30 Bar, is present at the end of the pressure tube, separated from the damper fluid by way of a floating piston. Expansion and compression of this gas volume compensates for the differing volumetric changes encountered in bump and rebound strokes as a result of the piston rod's presence in the rebound chamber. Several valve assemblies are present on the piston, one for compression and one for extension strokes.

The flow path architecture of these valves are outlined in Figure 1. For low damper velocities the preloaded blow-off valve remains closed and the net pressure/flow characteristic can be described by the series combination of the port channel and the fixed bleed. For higher velocities the blow-off valve progressively opens thus reducing the rate of increase of damper force with respect to velocity.

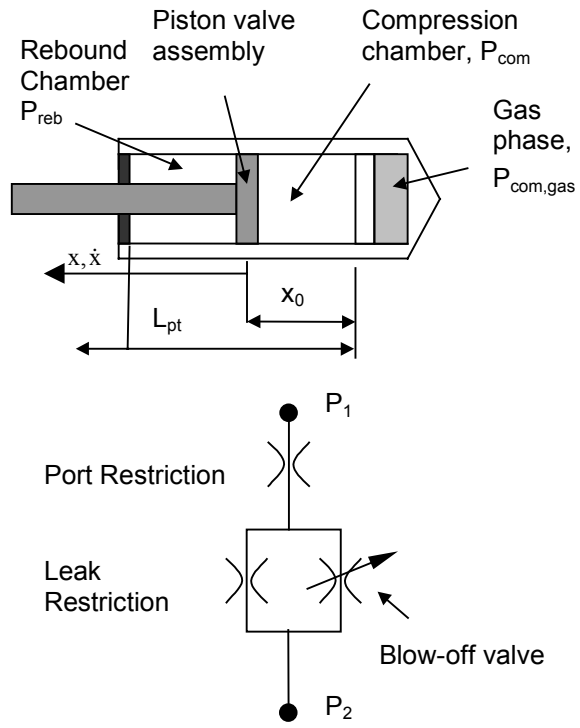


Figure 1. Mono-tube layout / axis system (top), and flow path architecture (bottom).

## MONO-TUBE DAMPER MODEL

The twin-tube damper model presented in [11-13] is a compressible model which is used solely for the purpose of simulations. To yield a readily identifiable damper model the parameters of the compressible model of [11-13] were identified by fitting an additional incompressible model to experimental data from which the hysteresis had been removed as described in [16,17]. As a result of the differing model architectures the pressure/flow model, required for the parameter identification processes, was different to that of the full compressible model. In this paper a single pressure/flow model will be derived for a mono-tube shock absorber for the parameter identification process, and the valve pressure/flow characteristics will then be supplied to the compressible damper model in the form of a simple look-up table. This modelling approach should yield more rapid simulations and additional robustness without compromising model tune-ability. As will be discussed later this can also yield improvements in model accuracy and flexibility; for non-standard valve architectures it will now only be necessary to derive a single new pressure/flow model.

PRESSURE MODEL -The contribution of the damper oil's compressibility to the hysteretic nature of shock absorbers dynamic behaviour is modelled with the assumption that the relative change in oil volume is proportional to pressure:

$$\frac{V_0 - V}{V_0} = \alpha p \tag{1}$$

The mono-tube pressure model consists of a first order non linear differential equation, (2), derived from (1) for the rebound chamber and a simple relationship from the adiabatic gas law which relates the compression chamber pressure to piston position (3).

$$\frac{dp_{reb}}{dt} = \frac{(\dot{x}(A_{pt} - A_{rod}) - Q_{pv})(1 - \alpha p_{reb})}{(L_{pt} - x_0 - x)(A_{pt} - A_{rod})\alpha} \tag{2}$$

$$P_{com} = P_{gas,static}\left(\frac{V_{gas,static}}{V_{gas,static} + A_{rod}x}\right)^{\gamma} \tag{3}$$

Assuming a simple Coulomb friction model the damper force is thus given by:

$$F_{damper} = (A_{pt} - A_{rod})P_{reb} - A_{pt}P_{com} + F_{friction}\,sgn\dot{x} \tag{4}$$

For a full derivation of (2) the reader is referred to [13].

INCOMPRESSIBLE MONO-TUBE DAMPER MODEL -In this section an incompressible mono-tube damper model will be derived that evaluates damper control force as a function of velocity, utilising the axis system and sign conventions detailed in Figure 1. The model structure is very similar to that presented in [11-13] for a twin-tube shock absorber.

CALCULATION OF THE VALVE FLOW RATES - Since the damper hydraulic fluid is assumed to be incompressible the rebound chamber volume may be directly determined at any time increment from the damper's geometry.

$$V_{reb} = (L_{pt} - x_0 - x)(A_{pt} - A_{rod}) \tag{5}$$

Differentiation of this expression yields an expression for the rate of change of the chamber volume with respect to time:

$$\dot{V}_{reb} = -\dot{x}(A_{pt} - A_{rod}) \tag{6}$$

From (6) it is thus possible to define the flow rates through the individual damper valves to the defined sign convention:

$$\begin{aligned} Q_{tot,reb\rightarrow com} &= -\dot{V}_{reb} = \dot{x}(A_{pt} - A_{rod}) \\ Q_{tot,com\rightarrow reb} &= -(Q_{reb\rightarrow com}) = -\dot{x}(A_{pt} - A_{rod}) \end{aligned} \tag{7}$$

VALVE PRESSURE/FLOW CHARACTERISTICS -The individual valve characteristics of the port and leak restrictions can be characterised by simple power law expressions. An exponent of 1.75 was proposed by Reybrouck [18] and shown to be accurate for a range of damper valves [11-13,15-17].

$$\Delta P_{port} = K_{port}\nu^{1/4}Q_{port}^{\ 7/4} \tag{8}$$

$$\Delta P_{leak} = K_{leak}\nu^{1/4}Q_{leak}^{\ 7/4} \tag{9}$$

The blow-off valve pressure/flow characteristic is modelled as a function of two independent parameters, $\Delta P_0$, the pressure required to overcome the valve pre-load and the subsequent valve stiffness, $K_{spring}$. This expression is a simplified version of that utilised by Lang [9,10] proposed by Duym et al [11,17].

$$K_{spring}Q_{blow-off} = (\Delta p_{blow-off} - \Delta p_o)\sqrt{\Delta p_{blow-off}} \tag{10}$$

The total valve characteristics are represented as a combination of the individual valve characteristics in series and in parallel. For two valves in series the pressure drop over the total valve is the sum of the individual pressure drops and the flow through each is equal. For a parallel combination the total flow is the sum of the flow through each component and the pressure drops are equal:

$$\Delta p_{tot} = \Delta p_{leak} + \Delta p_{port} \tag{11}$$

Substitution of the port's pressure/flow characteristic, (8), yields:

$$\Delta p_{tot} = K_{port}\nu^{1/4}Q_{port}^{\ 7/4} + \Delta p_{leak} \tag{12}$$

The port flow can then be described as the sum of the leak and blow-off flows:

$$\Delta p_{tot} = K_{port}\nu^{1/4}\left(Q_{leak} + Q_{blow\ off}\right)^{7/4} + \Delta p_{leak} \tag{13}$$

While the blow-off valve remains closed the leak flow equals the total flow. Inserting this into (9) yields:

$$\Delta P_{leak}\big|_{closed} = K_{leak}\nu^{1/4}Q_{tot}\big|_{closed}^{\ 7/4} \tag{14}$$

Substituting this expression into (13), and for zero blow-off valve flow thus yields an explicit relationship for the pressure drop across a closed valve as function of flow rate:

$$\Delta p_{tot}\big|_{closed} = \left(K_{port} + K_{leak}\right)\nu^{1/4}\left(Q_{tot}\big|_{closed}\right)^{7/4} \quad (15)$$

For 2 individual valves in parallel:

$$Q_{tot} = Q_{leak} + Q_{blow-off} \quad (16)$$

Rearranging (16) to gain an expression for $Q_{blow-off}$ and substituting into (10) yields:

$$K_{spring}\left(Q_{tot}\big|_{open} - Q_{leak}\big|_{open}\right) = (\Delta p_{blow-off} - \Delta p_o)\sqrt{\Delta p_{blow-off}} \quad (17)$$

For 2 individual valves in parallel the pressure drop is the same across each element, therefore for pressures greater than the blow-off pressure, $\Delta P_{leak}$ is equal to $\Delta P_{blow-off}$. Substituting this into (9) leads to the following expression:

$$\Delta P_{blow-off} = K_{leak}\nu^{1/4} Q_{leak}\big|_{open}^{7/4} \quad (18)$$

Combination of (17) and (18) yields an explicit relationship for the total open valve flow in terms of the leak flow:

$$Q_{tot}\big|_{open} = Q_{leak}\big|_{open} + \frac{(K_{leak}\nu^{1/4} Q_{leak}\big|_{open}^{7/4} - \Delta p_o)\sqrt{K_{leak}\nu^{1/4} Q_{leak}\big|_{open}^{7/4}}}{K_{spring}} \quad (19)$$

AN EXPLICIT OPEN VALVE CHARACTERISTIC - In order to avoid an iterative numerical solution of (19), to determine the leak flow rate for a given total flow rate, the right hand side of (19) is expanded into a Taylor series about the blow off point, i.e. $Q_{leak} = Q_{leak,blow-off}$:

$$Q_{tot} = \sum_{i=0}^{3} B_i \left(Q_{leak}\big|_{open} - Q_{leak,blow-off}\right)^i \quad \text{for} \quad Q_{leak} > Q_{leak,blow-off} \quad (20)$$

with:

$$B_i = \frac{1}{i!}\frac{\partial^i}{\partial Q_{leak}\big|_{open}^{\,i}} Q_{tot}\big|_{open}\left(Q_{leak}\big|_{open}\right)\Bigg|_{Q_{leak}=Q_{leak,blow-off}} \quad (21)$$

The derived Taylor series coefficients are given in Appendix 1.

A third order Taylor series expansion yields a cubic equation which can then be solved utilising Cardano's rule [19]. The Cardano coefficients are presented in Appendix 2. The resulting explicit representation for the leak flow is as follows:

$$Q_{leak}\big|_{open} = Q_{leak,blow-off} - \frac{B_2}{3B_3} + \sqrt[3]{-\frac{D_2}{2} + \sqrt{D_3}} + \sqrt[3]{-\frac{D_2}{2} - \sqrt{D_3}} \quad (22)$$

Now at the blow-off point $\Delta P_{leak}$ is equal to $\Delta P_0$. Rearranging (9) and inserting this condition yields:

$$Q_{leak,blow\ off} = \left(\frac{\Delta p_0}{K_{leak}\nu^{1/4}}\right)^{4/7} \quad (23)$$

From (9) the pressure drop across a leak restriction for open blow-off valve flow is given by:

$$\Delta P_{leak}\big|_{open} = K_{leak}\nu^{1/4} Q_{leak}\big|_{open}^{7/4} \quad (24)$$

The pressure drop over the port restriction is then calculated using (8). Noting that the flow through the port restriction is equal to the total flow:

$$\Delta P_{port}\big|_{open} = K_{port}\nu^{1/4} Q_{tot}\big|_{open}^{7/4} \quad (25)$$

The total pressure drop over the valve assembly is then obtained by adding the pressure drops of the series combination of individual valves:

$$\Delta p_{tot}\big|_{open} = \Delta p_{leak}\big|_{open} + \Delta p_{port}\big|_{open} \quad (26)$$

Substituting (24) and (25) into (26) yields the final expression for the total pressure drop over an open valve assembly:

$$\Delta p_{tot}\big|_{open} = \nu^{1/4}\left(K_{leak} Q_{leak}\big|_{open}^{7/4} + K_{port} Q_{tot}\big|_{open}^{7/4}\right) \quad (27)$$

A SMOOTHED BLOW-OFF CHARACTERISTIC - The outlined model results in a sharp transition between 'closed valve' and 'open valve' operating scenarios when viewed on a pressure/flow diagram. In reality this transition between regimes is rounded off possibly due to leakage through the blow-off valve prior to the blow-off condition being met. The following empirical formula is thus utilised to provide a smoothing effect:

$$\Delta p_{smooth} = \frac{\Delta p_{tot}\big|_{open} \times \Delta p_{tot}\big|_{closed}}{\sqrt[G]{\left|\Delta p_{tot}\big|_{open}\right|^{G} + \left|\Delta p_{tot}\big|_{closed}\right|^{G}}} \quad (28)$$

For a closed blow-off valve the Taylor series approximation cannot be utilised to represent the pressure drop over an open valve hence the explicit characteristic given by (22) and (27) is linearly extrapolated at the blow-off point as follows:

$$\Delta p_{tot}\big|_{open} = H_0 + H_1(Q_{tot} - B_0) \quad (29)$$

Where $H_0$ and $H_1$ are the extrapolation coefficients defined in appendix 3.

For the compressible damper model of Duym [11-13], where the valve flows are calculated as a function of pressure drop, it is necessary to smooth the calculated flow, as opposed to pressure, and with an alternative empirical formula to that used in the incompressible model(28). As such this is a possible source of inaccuracy when switching between the models.

THE DAMPER FORCE - As a result of the differing areas in the rebound and compression chambers a static force exists at rest which is given by the following equation:

$$F_{static} = -A_{rod} P_{gas,static} \quad (30)$$

In order to facilitate the parameter identification process the compression chamber pressure is assumed to remain constant at the static gas pressure, $P_{gas,static}$. Therefore:

$$P_{reb} = \Delta p + P_{gas,static} \quad (31)$$

Substitution of (31) with (30) into (4) yields the desired expressions for the damper force:

$$\begin{aligned} F_{rebound} &= F_{static} + \Delta p(A_{pt} - A_{rod}) + F_{friction}\,\mathrm{sgn}\,\dot{x} \\ F_{compression} &= F_{static} - \Delta p(A_{pt} - A_{rod}) + F_{friction}\,\mathrm{sgn}\,\dot{x} \end{aligned} \quad (32)$$

## PARAMETER IDENTIFICATION

For the current paper the same parameter identification approach was taken to that of Duym et al [12,13,17]. This approach will be briefly introduced here. Experimental data was collected from two dynamometer tests. The first being a quasi-static test, where the shock absorber was extended and compressed at a constant low velocity. For the second test the shock absorber was excited by a sine chirp signal.

The parameter values were then determined through the process of least squares minimisation. Optimisation routines were implemented in Matlab (v5.3) using the sub routine, Lsqnonlin, which is provided within the optimisation toolbox. At each time increment, $t_i$, for a set of parameters, P, and for N samples of experimental data the squared difference between the modelled output of interest, $U_{modelled}$, and the corresponding experimental input, $U_{measured}$, was evaluated with respect to a set of experimental inputs, $I_{measured}$ viz:

$$C(P) = \sum_{i=1}^{N}\left[\begin{matrix} U_{modelled}(t_i, I_{measured}(t_i), P) \\ -(U_{measured}(t_i, I_{measured}(t_i)) \end{matrix}\right]^2 \quad (33)$$

The model parameters, P, were thus optimised to minimise the function, C.

To facilitate an efficient optimisation process the Jacobian of the modelled signal was derived and implemented into the optimisation routines. If the experimental data, to which the model is to be fitted, is a matrix of m components and n is the number of parameters then the Jacobian, J, is an m-by-n matrix where J( i, j ) is the partial derivative of $U_{modelled}(i)$ with respect to P(j). Explicitly defining the Jacobian makes the optimisation process more rapid simply due to the fact that if the Jacobian is not supplied it has to be evaluated numerically which is more costly in terms of time.

A simple measure of model fit quality is given by the RMS of the residual signal viz.

$$\text{RMS of the residual} = C_{RMS} = \sqrt{\frac{C}{N}} \quad (34)$$

A relative measure of the fit quality can also be obtained by comparing the residual RMS to the RMS value of the measured signal:

$$\text{Relative RMS of Residual} = \frac{C_{RMS}}{U_{Measured-RMS}} \quad (35)$$

QUASI-STATIC TEST - For the selected test velocity of 4mms$^{-1}$ the generated damper force was assumed to consist of little viscous damping and could thus be attributed to the compression/expansion of the gas volume contained within the shock-absorber and due to friction. To ensure that this assumption was valid the quasi static test was also performed for the 'comfort' and 'normal' settings of the prototype shock absorber. A comparison of these softer damper settings to that of the 'sport' setting showed little variation in results between the three. Assuming the pressures are equal in each of the three chambers the following applies:

$$F = P_{com}(A_{pt} - A_{rod}) - P_{com}A_{pt} + \mathrm{sign}(\dot{x})F_{friction} \quad (36)$$

Simplifying and applying the reserve chamber isentropic law based function (3) yields:

$$F = -A_{rod} P_{gas,static} \left( \frac{V_{gas,static}}{V_{gas,static} + A_{rod} x} \right)^{\gamma} + \text{sign}(\dot{x}) F_{friction} \quad (37)$$

The static gas pressure and volume and friction value were thus identified from (37) and experimental data using the aforementioned technique of least squares minimisation. Figure 2 shows the predicted and measured force/displacement characteristics. The calculated value for the RMS of the residual was 6.7 N, indicating a close match has been obtained.

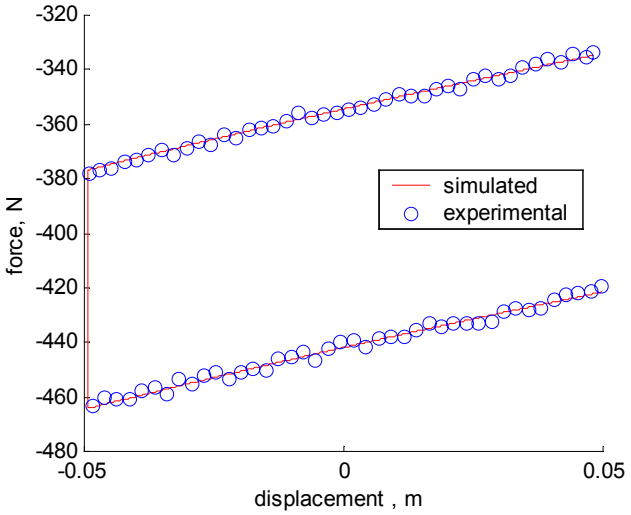


Figure 2 . Quasi-static test/simulation results (sport)

SINE CHIRP EXCITATION TEST - The parameters for the incompressible model were optimised using the previously defined techniques using data obtained from a 'modified' sine chirp excitation signal. The chirp signal shown in Figure 3 was utilised, as in [11-13,17], so that the required frequency range would be swept through exponentially preventing prolonged excitation at elevated velocities. Hysteresis was consequently removed from the experimental data, prior to the parameter identification process, by only retaining data where velocity and acceleration had different signs. For an in depth description of the hysteresis 'filtering' and data pre-processing steps taken the reader is referred to [17]. Figure 4 shows a plot of the resulting force/velocity data superimposed with that predicted by the incompressible damper model. As can be seen the incompressible model matches the experimental data closely.

## VALIDATION OF MONO-TUBE DAMPER MODEL

In order to validate the described damper model the output characteristics of interest were simulated for sinusoidal excitations of 1, 3 and 12 Hz. All of the sine wave amplitudes were 0.05m with exception of the 12 Hz signal which was 0.005m. These simulated results were then compared to those obtained from experiment for identical excitation signals.

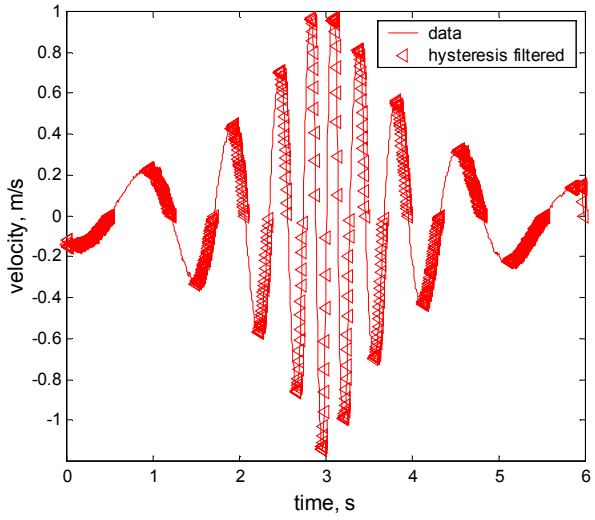


Figure 3. Velocity/time plot for chirp signal, and corresponding plot with hysteresis removed.

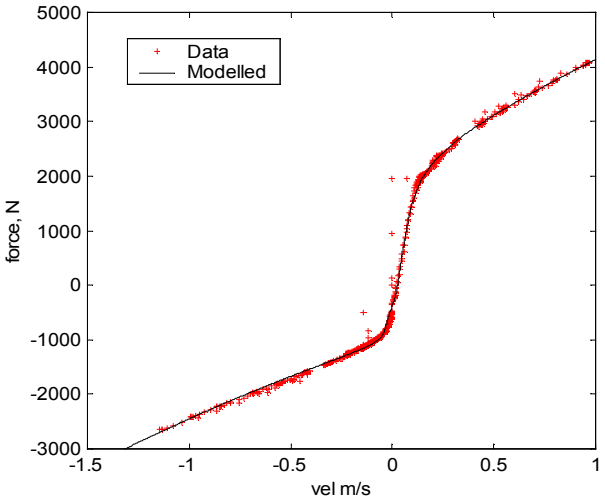


Figure 4. Experimental force/velocity identification data with hysteresis removed overlaid with incompressible damper model prediction.

Looking at Figure 5 it can be seen that the simulated curves match the experimental data very well for each of the three frequencies of excitation that were evaluated.

All of the parameter values listed in Figure 6 are either identified from the two experimental procedures or gathered from manufacturers data such as the geometry based parameters. At present the only parameter that is not identified experimentally or taken directly from data sheets is the one for compressibility, $\alpha$. In order to account for compliances other than that of the oil itself it is preferable to subtly adjust the value of oil compressibility which can be obtained from data sheets. For this study a value was taken of $1.5e^{-9}Pa^{-1}$.

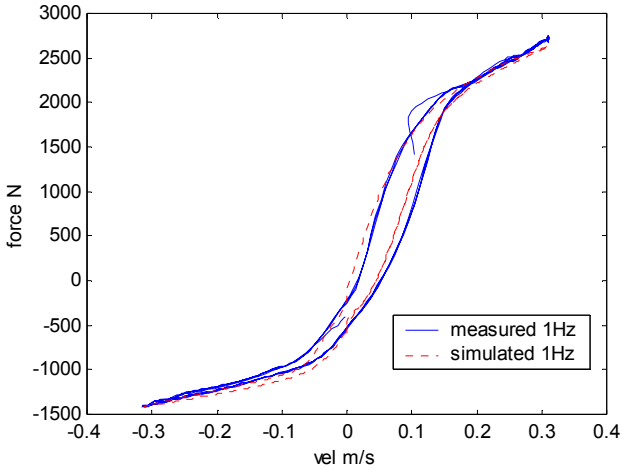


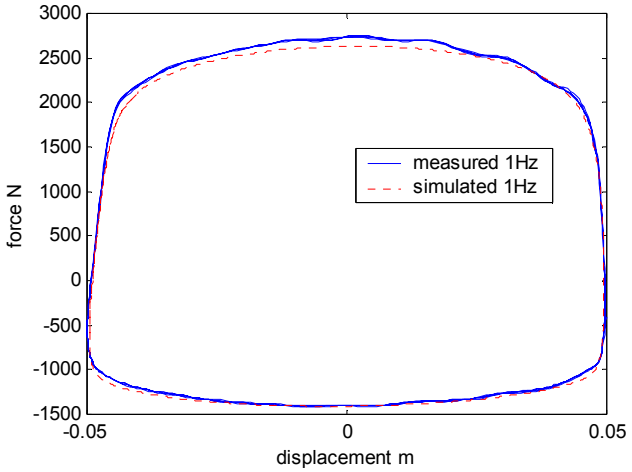


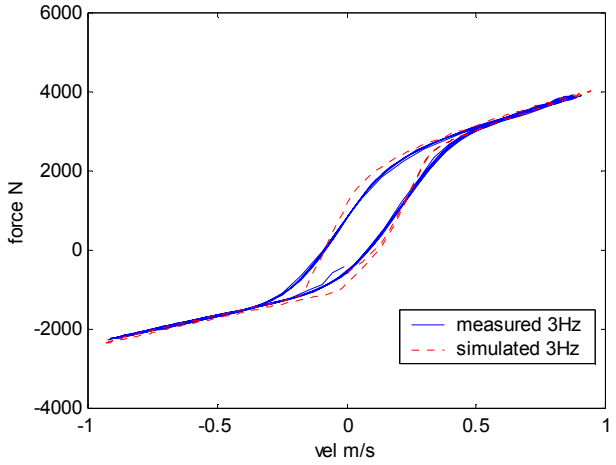


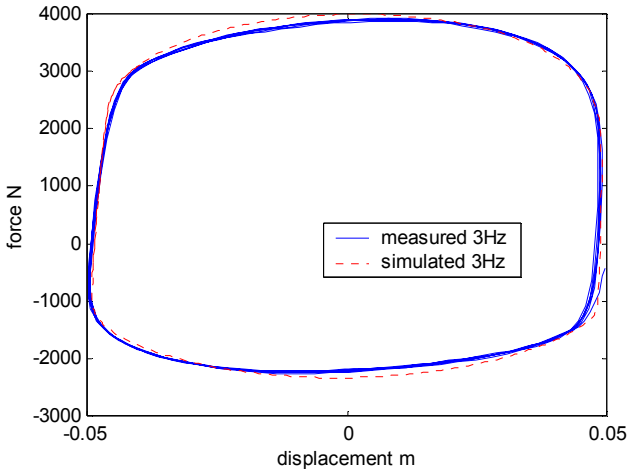


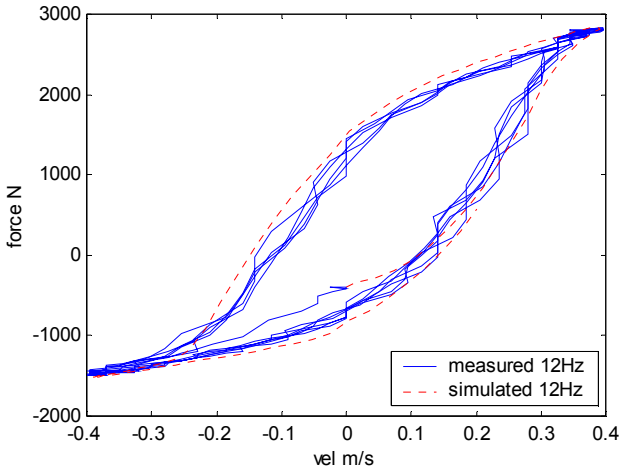


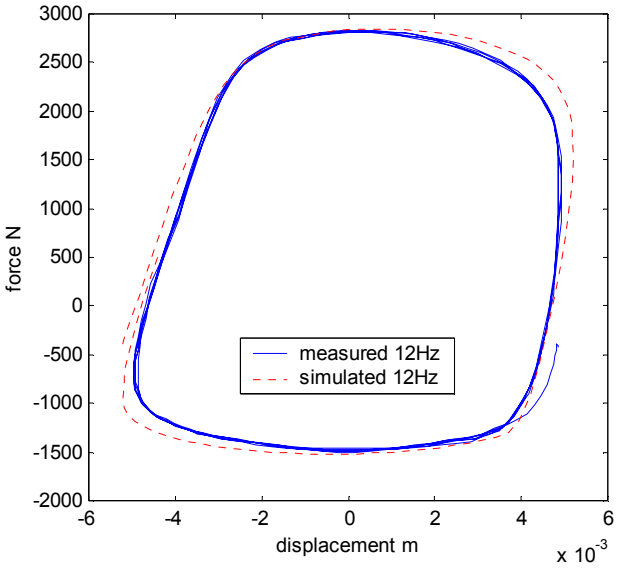


Figure 5. Experimental and simulated force/velocity and force/displacement plots for differing sinusoidal excitation frequencies.

| | Geometric/ data-sheet Parameters | Magnitude | Units |
|---|---|---|---|
| | $L_{pt}$ | 0.453 | m |
| | $X_0$ | 0.1355 | m |
| | $\phi_{rod}$ | 13e-3 | m |
| | $\phi_{piston}$ | 36e-3 | m |
| | $\gamma$ | 1.4 | N/A |
| | $\nu$ | 21e-6 | $m^2/s$ |
| Quasi-static identified parameters | Friction | 43.7 | N |
| | $V_{gas,static}$ | 1.2299e-4 | $m^3$ |
| | $P_{gas,static}$ | 2.9995e+6 | Pa |

| Identified Valve parameters | Compression | Rebound | Units |
|---|---|---|---|
| $K_{leak}$ | 6.54e+014 | 7.63e+014 | $kg/m^{27/4}$ |
| $K_{port}$ | 2.02e+012 | 1.20e+011 | $kg/m^{27/4}$ |
| $K_{spring}$ | 1.56e+012 | 6.50e+012 | $Kg^{3/2}/s^2m^{9/2}$ |
| $\Delta p_0$ | 6.82e+005 | 2.74e+006 | Pa |
| G | 1.7 | 1.5 | N/A |

Figure 6. Non-linear mono-tube damper model parameters.

## QUARTER CAR RIDE MODELLING

This section describes a simple investigation to quantify any improvements in accuracy that a hysteretic damper model might have on simulated vehicle behaviour when compared to simpler damper representations. The proposed damper model was incorporated into a classical vehicle quarter car ride model, Figure 7, and both time and frequency domain related characteristics were compared to those obtained with conventional 14 speed test and linear damper representations. To ensure a fair comparison for this section the 14 speed test was simulated from the non-linear damper model, and not performed experimentally. In this way the investigation may be carried out in isolation of the effects of slight inaccuracy of the hysteretic damper model compared to actual characteristics. The purpose of this section is to identify the need for a hysteretic damper model but, clearly there is also a requirement to validate the exact improvements that the proposed damper model offer when compared to conventional representations by comparisons to vehicle objective data. In order to ensure that the comparative study focuses on variations between the overall damper modelling approaches, the 14 speed test approach was also simulated for an elevated number of test frequencies to eliminate inaccuracies/variations due to exact frequency selection and as a result of a 28 point fit to a force/velocity curve .

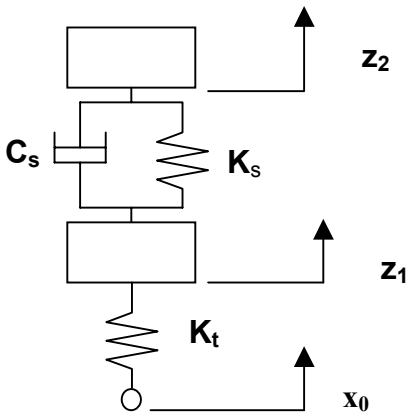


Figure 7. Quarter car ride model.

The equations of motion for the quarter car model shown in Figure 7 are:

$$\begin{aligned} M_w\ddot{z}_1 &= K_t(x_0 - z_1) - K_s(z_1 - z_2) - C_s(\dot{z}_1 - \dot{z}_2) \\ M_b\ddot{z}_2 &= K_s(z_1 - z_2) + C_s(\dot{z}_1 - \dot{z}_2) \end{aligned} \quad (38)$$

The input parameters for this model are outlined in Figure 8.

Two types of road surface input were applied to the quarter car model, one representing a length of simulated road, and one of a standard feature, namely a pothole. Time domain results were recorded and then converted to the frequency domain in the case of the 'random road' in order to evaluate weighted RMS vertical body accelerations according to ISO 2631 [21].

| Parameter | Magnitude | Units |
|---|---|---|
| $M_w$ | 55.5 | kg |
| $M_b$ | 451.8 | kg |
| $K_t$ | 250 | kN/m |
| $K_s$ (Wheel rate) | 29.7 | kN/m |
| $C_s$ (Damper rate) | 2622 | Ns/m |
| Damper Motion Ratio | 1.5 | N/A |

Figure 8. Parameters for quarter car ride model (Front)

RANDOM ROAD INPUT MODELLING - For this study a time dependant road profile was derived from a spectral density road description, defined in terms of frequency, in cycle/s, as described by Crolla et al [20]. The spectral density is given by the following simple formula, where G is a roughness coefficient, V is vehicle speed in m/s and p is equal to the gradient of the log-log spectral density curve:

$$S(f) = \frac{GV^{p-1}}{f^{p}} \qquad (39)$$

For the first section of this study a vehicle speed of 45mph (20m/s) was selected along with typical values for a minor road of roughness coefficient of $5x10^{-6}$, and an index p value of 2.5.

The linear damper rate, given in Figure 8, was carefully selected to yield an equivalent compromise between RMS Dynamic Tyre Load (DTL) variation and RMS weighted vertical body acceleration (ACC), to that of the non-linear hysteretic damper model, for the defined vehicle speed of 20m/s. The damper rate selected is slightly softer than that required to minimise DTL for this condition.

Figure 9 shows the predicted time histories for Suspension Working Space (SWS), which is given by $z_1$-$z_2$, for each damper representation, for the initial 2 seconds of simulation. An interesting feature is that the linear damper predictions are generally vertically offset relative to each of the other two damper representations. This general trend is maintained for the full length of simulated road of 500m. This offset yields a lower peak value of SWS in damper compression and a higher value in extension compared to the other damper representations, see Figure 10. This is clearly a manifestation of the effect of asymmetric damping for the 14 speed and modelled dampers, with rebound being higher than bump.

A further interesting result is that for similar predicted weighted vertical body accelerations and RMS SWS values the modelled non-linear hysteretic damper model predicts a RMS DTL variation of 6% less than that for the 14 speed test representation with peak DTL's some 10% lower.

Figure 11 shows the variation of the discomfort parameter, ACC, for each of the damper models, for a range of vehicle speeds over the defined typical minor road. The linear damper curve intersects the modelled damper curve in the region of 20 m/s. This is to be expected due to the method chosen to select the linear damper rate. It can be seen that the discrepancy between the predicted ACC values for the linear damper and the other two representations are proportional to the percentage speed increase or decrease relative to this point. Again this trend is to be expected since for higher vehicle speeds, and hence damper velocities, the linear damper will provide higher forces and hence ACC values and vice versa for lower vehicle speeds.

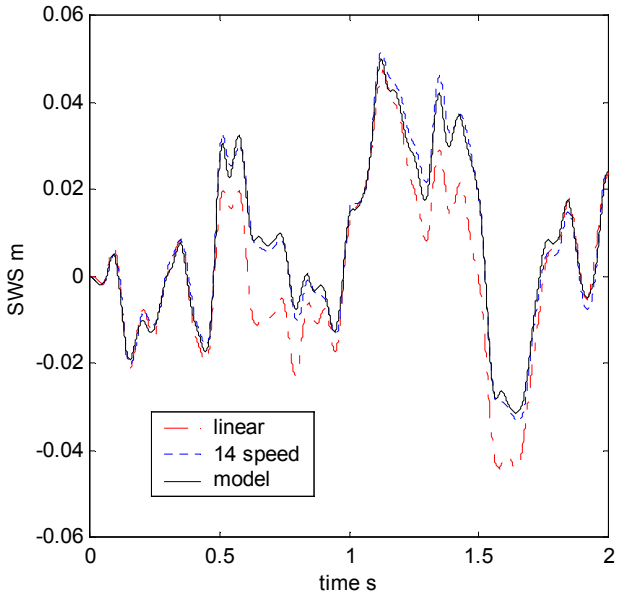


Figure 9. Simulated SWS versus time for first 2 seconds of 500m of typical minor road being traversed at 20m/s, for three differing damper representations.

| | Units | Linear damper | 14 speed damper | Non-linear damper |
|---|---|---|---|---|
| SWS (RMS) | m | 0.026 | 0.028 | 0.028 |
| Weighted Body accel (RMS) | $m/s^2$ | 2.26 | 2.29 | 2.33 |
| DTL (RMS) | | 1.63 | 1.69 | 1.59 |
| Peak SWS | m | 0.078<br>-0.091 | 0.091<br>-0.079 | 0.091<br>-0.079 |
| Peak body accelerations | $m/s^2$ | 8.52<br>-10.50 | 7.92<br>-9.72 | 8.02<br>-9.67 |
| Peak DTL | kN | 5.18<br>-5.68 | 5.86<br>-5.85 | 5.33<br>-5.47 |

Figure 10. Simulated RMS and Peak output values for 20m/s simulation over 500m of typical minor road for three differing damper representations.

When comparing the outputs obtained for the 14 speed test damper to the non-linear hysteretic damper model several overall trends are displayed. For low vehicle speeds the predicted discomfort parameter is similar, however for higher speeds there is more variation. Generally for all speeds the damper model predicts higher ACC values than the 14 speed damper.

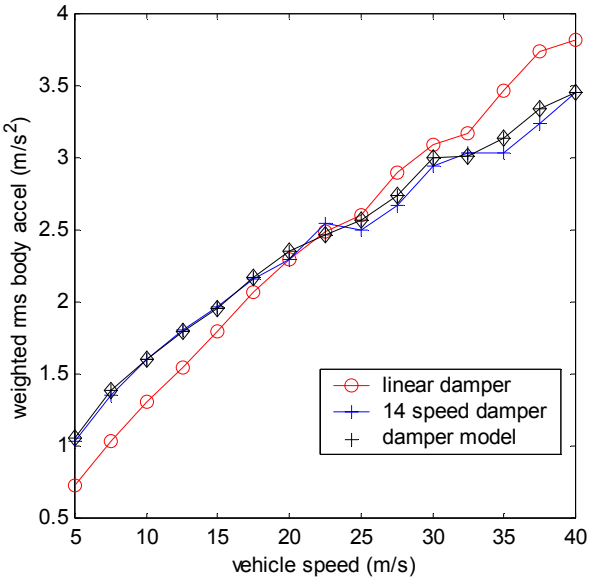


Figure 11. Discomfort parameter versus vehicle speed for three differing damper models traversing a typical minor road.

STANDARD FEATURE - A pothole matching the geometry of that given in Figure 12 was applied as the road input to the quarter car ride model. This is an example of a standard pothole that is used by Jaguar for test work at MIRA [20].

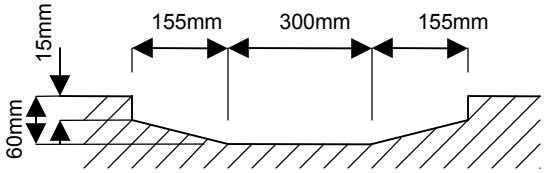


Figure 12. Standard pothole geometry.

For this investigation a vehicle speed of 10 m/s was selected.

The simulated peak and RMS values for suspension working space, body acceleration, and tyre load variation are given in Figure 13, and time histories for each of these outputs in Figure 14. Interestingly from Figure 13 it can be seen that the non-linear damper predicts peak values for both DTL and body acceleration of approximately 10% and 3% smaller for tyre compression and extension respectively than that of the 14 speed damper. This is for an increase in predicted RMS SWS of the order of 2% and peak value of 1%. The output characteristics displayed for the linear model damper model, in terms of RMS and peak values, differ significantly from those of the other damper representations, and indicate higher levels of overall damping. This finding correlates well with the results of the investigation of the effects of differing road speeds on discomfort parameter for a minor road, see Figure 11; at higher velocities a linear damper provides higher levels of damping relative to the other two damper representations.

| | Units | Linear damper | 14 speed damper | Non-linear damper |
|---|---|---|---|---|
| SWS (RMS) | m | 0.0325 | 0.04201 | 0.0430 |
| Body accel (RMS) | $m/s^2$ | 8.21 | 6.62 | 6.52 |
| DTL (RMS) | kN | 5.51 | 6.66 | 6.55 |
| Peak SWS | m | 0.0416<br>-0.0624 | 0.0670<br>-0.0715 | 0.0683<br>-0.0733 |
| Peak body acceleration | $m/s^2$ | 17.85<br>-14.41 | 11.37<br>-11.30 | 10.52<br>-11.094 |
| Peak DTL | kN | 15.31<br>-11.184 | 14.87<br>-11.255 | 14.03<br>-10.977 |

Figure 13. RMS and Peak output values for 10m/s simulation over a typical pothole for three differing damper representations.

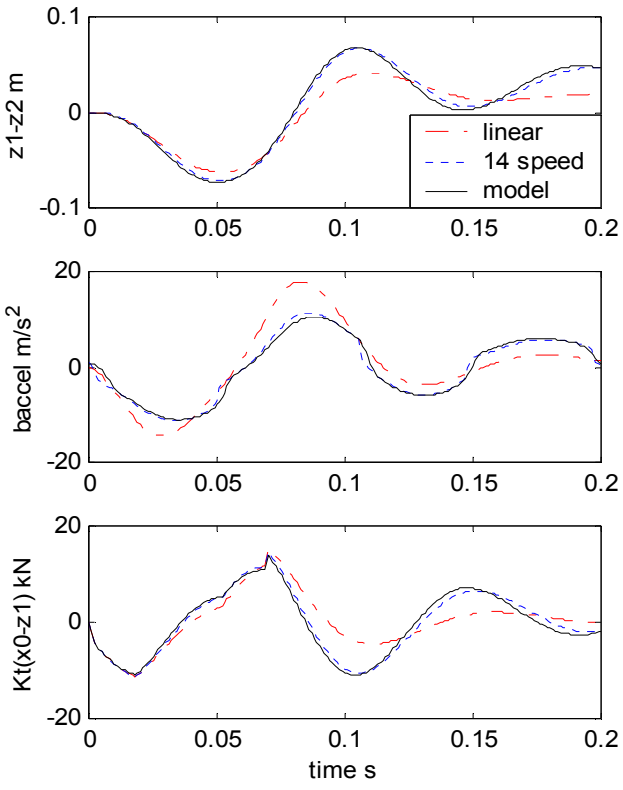


Figure 14. Simulated time histories for 10m/s simulation over a pothole for three differing damper representations.

## CONCLUSIONS

The parameters of a relatively complex non linear damper model have been successfully extracted, in an automated fashion, from data obtained from two simple experimental procedures. The model has been successfully validated to a high degree of accuracy by comparing simulated results to experimental data for 3 discrete frequencies of sinusoidal excitation of 1,3, and 12Hz.

The differences between simulated vehicle ride output characteristics for the non-linear damper model and several simpler damper representations have been investigated for a simple 2 d.o.f quarter car ride model. This work has indicated that gains to vehicle modelling accuracy may be achieved by utilising the derived damper model in preference to a 14 speed representation and has also identified the inadequacy of a single linear damper rate to accurately predict vehicle outputs over a broad range of operating conditions.

Future work will investigate the effects of improved friction representations within the damper model in the context of vehicle dynamics. The damper model will also be incorporated into vehicle models of elevated complexity and a case study will be performed of the adaptive damping strategy for the vehicle introduced within this paper. Further work is also needed to validate the findings of the vehicle ride modelling work carried out within this paper.

## ACKNOWLEDGMENTS

This research is sponsored by RICARDO VEHICLE ENGINEERING as part of an ongoing project to deliver an improved systematic methodology for the early development of damper properties to influence the ultimate ride and handling properties of vehicles.

## REFERENCES

1. Richardson, C. Ride Manual. Monroe Europe.
2. Belingardi, G. and Campanile, P. Improvement of the Shock Absorber Dynamic Simulation by the Restoring Force Mapping Method. Proceedings of the 15th International Modal Analysis Conference, Leuven, Belgium, pp. 441-454, Sep 1990.
3. Audenino, A. and Belingardi, G. An Application of the Restoring Force Mapping Method for the Diagnostic of Vehicular Shock Absorbers Dynamic Behaviour. Proc 2nd. Int. Machinery Monitoring and diagnostics conference, LA, California, pp.560-566, 1990.
4. Duym, S., Schoukens, J. and Guillaume, P. A Local Restoring Force Surface Method. Proceedings of the 13th International Modal Analysis Conference , Nashville, Tennessee, pp. 1392-1399, 1995.
5. Cafferty, S., Worden , K. and Tomlinson, G. R. Characterisation of Automotive Shock Absorbers Using Random Excitation. Proc Instn Mech Engrs, Vol 209, Part D, pp. 239-248, 1995.
6. Fash, J. Modeling of Shock Absorber Behaviour using Artificial Neural Networks. SAE paper 940248, 1994.
7. Besinger, F. H., Cebon, D. and Cole, D. J. Damper Models for Heavy Vehicle Ride Dynamics. Vehicle System Dynamics, 24, pp. 35-64, 1995.
8. Willumeit, H.P. and Tong, Z. Investigation of the high frequency disturbance response of vehicle suspension. FISITA Congress, IMechE, London, pp. 319-327, 1992.
9. Lang, H.H. A Study of the Characteristics of Automotive Hydraulic Dampers at High Stroking Frequencies, PhD Dissertation, The University of Michigan, 1977.
10. Segel, L. and Lang, H.H. The Mechanics of Automotive Hydraulic Dampers at High Stroking Frequencies. Vehicle System Dynamics 10, pp. 82-85, 1981.
11. Duym, S. Simulation Tools, Modelling and Identification, for an Automotive Shock Absorber in the Context of Vehicle Dynamics, MDI conference, France, 1998.
12. Duym, S. and Reybrouck, K. Physical Characterisation of Nonlinear Shock Absorber Dynamics. European Journal of Mechanical Engineering, Vol. 43, No4, pp. 181-188, 1998.
13. Reybrouck, K. and Duym, S. A Physical and Parametric Model for Nonlinear Dynamic and Temperature–Dependant Behaviour of Automotive Shock Absorbers. Proceedings of the 11th ADAMS Users Conference, Frankfurt.
14. Lang, R, and Sonnenburg, R. A Detailled Shock absorber Model for Full Vehicle Simulation., presented at the 10th European ADAMS Users' Conference, Frankfurt, Germany, November 14-15, 1995.
15. Herr, F., Mallin, T. and Roth, S. A Shock Absorber Model Using CFD Analysis and Easy5. SAE Steering and Suspension Technology Symposium 1999, p.p. 267-281, 1999.
16. Duym, S. Stiens, R. and Reybrouck, K. Fast Parametric and Nonparametric Identification of Shock Absorbers. Proc. 21st INT. Seminar Modal Analysis Noise and Vibration Engineering Conference. Leuven, pp. 1157-69, 18-20 Sep 1996.
17. Duym, S., Stiens, R. and Reybrouck, K. Evaluation of Shock Absorber Models. Vehicle system dynamics, 27, pp. 109-127, 1997.
18. Reybrouck, K. A Non Linear Parametric Model of an Automotive Shock Absorber, SAE International Congress, Detroit, Michigan, February 28- March 3, pp. 79-86, 1994.
19. Cardano, G. Ars Magna, Nuremberg, 1545.
20. Crolla, D.A., Firth, G., Horton, D. An Introduction to Vehicle Dynamics. Internal University of Leeds document pp. 12.
21. International Standard ISO 2631-1:1997, Mechanical Vibration and Shock – Evaluation of Human Exposure to Whole Body Vibration – Part 1: General Requirements.

## CONTACT

Adrian Simms. menajs@leeds.ac.uk

## DEFINITIONS

**Compressible damper model:** A damper model which models effects of damper internal compliances to yield hysteretic dynamic behaviour.

**Incompressible damper model:** A damper model which assumes damper internal compliances are negligible, and that control force is related solely to damper velocity; hence non-hysteretic behaviour is predicted.

## APPENDIX 1.

The Taylor Coefficients:

$$B_0 = Q_{leak,blow-off} \tag{40}$$

$$B_1 = 1 + \frac{7\sqrt{\Delta p_0{}^3}}{4K_{spring}Q_{leak,blow-off}} \tag{41}$$

$$B_2 = \frac{35\sqrt{\Delta p_0{}^3}}{16K_{spring}Q_{leak,blow-off}{}^2} \tag{42}$$

$$B_3 = \frac{217\sqrt{\Delta p_0{}^3}}{512K_{spring}Q_{leak,blow-off}{}^3} \tag{43}$$

## APPENDIX 2.

The Cardano Coefficients:

$$D_1 = \left(\frac{3B_1B_3 - B_2{}^2}{3B_3{}^2}\right) \tag{44}$$

$$D_2 = \frac{2B_2{}^3 - 9B_1B_2B_3 + 27(B_0 - Q_{tot})B_3{}^2}{27B_3{}^3} \tag{45}$$

$$D_3 = \frac{D_2{}^2}{4} + \frac{D_1{}^3}{27} \tag{46}$$

## APPENDIX 3.

Linear extrapolation coefficients:

$$H_0 = B_0{}^{7/4}\nu^{1/4}(K_{leak} + K_{port}) \tag{47}$$

$$H_1 = \left.\frac{\Delta p_{tot}|_{open}}{dQ_{tot}}\right|_{blow-off} = \frac{7\nu^{1/4}B_0{}^{3/4}}{4} \times \left(\frac{K_{leak}}{12B_3\sqrt{D_3}}\left(\begin{array}{l}\left(-\frac{D_2}{2} + \sqrt{D_3}\right)^{-2/3}(2 - D_2) + \\ \left(-\frac{D_2}{2} - \sqrt{D_3}\right)^{-2/3}(2 + D_2)\end{array}\right) + K_{port}\right) \tag{48}$$